

NMR State Diagram Concept

XIANGYANG LIN, ROGER RUAN, PAUL CHEN, MYONGSOO CHUNG, XIAOFEI YE, TOM YANG, CHRIS DOONA, AND TOM WAGNER

ABSTRACT: This article introduces a new concept, the NMR (nuclear magnetic resonance) state diagram, in the context of food shelf-life stability as affected by the molecular mobility of the food matrix. Our literature review shows that some shelf-life-related changes cannot be explained or predicted by the current a_w and glass transition temperature concepts. This article presents the theoretical principles and some experimental evidence of the NMR state diagram concept that could be complementary to the a_w and glass transition concepts. An NMR state diagram is a curve of NMR relaxation time versus temperature. Some of the curve features were found to correlate highly to the physiochemical states and changes of food polymers, for example, caking, stickiness, and firming. The potential applications of this concept in quality and safety of food products, especially dry and intermediate moist foods, may include ingredients screening, prediction of physiochemical changes, chemical degradation, and microbiological activity. The goal concept of this article is to provoke more in-depth studies to analyze the relationships among NMR relaxation, molecular mobility, and stability of foods.

Keywords: glass transition, NMR, nuclear magnetic resonance, shelf-life, state diagram

Introduction

The shelf stability of food products is thought to be closely related to their physiochemical properties (Noel and others 1990; Buera and Karel 1995; Roos and others 1996; Kilcast and Subramaniam 2000). In the last 2 decades, the relationship between food stability and glass transition, a concept originated from the polymer science field, has been extensively studied in the food science and technology community (Slade and others 1993; Rahman 2006). The glass transition concept describes transitions between the rubbery state and the glassy state in a polymer as the polymer experiences temperature rise or fall. The temperature at which the polymer undergoes transition is called glass transition temperature, or T_g . According to this concept, the polymer is most stable at and below its T_g . At the glassy state, the viscosity of polymer is so high that flow, deformation, reactive species diffusing, and colliding cannot take place or occur at extremely low rates. The concept also implies that the greater the difference between the T_g and the storage temperature above T_g , the faster the deterioration or reaction occurs. In addition, a decrease or an increase in water content or other plasticizers could take the polymer through the glass transition process.

A state diagram, which is a map of states of foods as a function of moisture content or solid content and temperature, consists of the glass transition curve as its center component along with the freezing curve, melting curve, and so on (Figure 1 [Rahman and others 2003]). State diagrams of foods help understand the changes in physiochemical properties when the foods are subjected to changes in water content/water activity and temperature. T_g values of many food products and ingredients have been established (Slade and others 1993). Many thermodynamic methods, including differential scanning calorimetry (DSC) and dynamic thermal analysis (DTA),

dynamic mechanical thermal analysis (DMTA), and dynamic mechanical analysis (DMA), have been used to analyze the glass-rubber transition. The key information obtained with these methods is the glass transition temperature.

The glass transition concept has proven very useful in understanding physical and structural properties of food polymers. However, in many cases, the glass transition concept alone does not predict shelf-life stability very well. Much experimental evidence does not support a clear correlation between T_g and microbial activity (Chirife and Buera 1994, 1995, 1996; Buera and others 1998; Vittadini and Chinachoti 2003). Similarly, many investigations show that glass transition alone cannot explain enzymatic and nonenzymatic activities below T_g . In some cases, reactions, for example, ascorbic acid oxidation, occur slower in the rubbery state than in the glassy state because the structural collapse in the rubbery state impeded O_2 diffusion through the system, which resulted in slower ascorbic acid degradation rates (Nelson 1994). However, the water activity concept, whose limitations (Rahman 2006) once made the glass transition concept popular, deserves another serious look in the face of chemical and biological stability of foods. More and more research has reevaluated the significance of water apart from being a plasticizer in the glass transition and found that water still plays a very important role in diffusion, microbial stability, enzymatic, and nonenzymatic reactions, and so on. Bell and Hageman (1994) conducted well-designed experiments to differentiate between the effects of water and glass transition on aspartame degradation in a solid system. They found that the rate of aspartame degradation depends on the water activity rather than the state of the system.

There are data showing high water mobility in the glassy state in foods. Roudaut and others (1999) studied the molecular mobility in low-moisture white bread as a function of temperature and found that the different motional processes involving water, side chains, and even the main chains are possible in the samples even below the glass transition temperature, which coincided with the fact that water was still mobile even in the glassy state. They concluded that T_g is not a universal predictive parameter for the physical stability of glassy food. Li and others (1998) found that in waxy corn starch, much of the water (> 50% of water present) remained very high in mobility even below -32°C , regardless of the relatively rigid starch

MS 20060301 Submitted 5/26/2006, Accepted 9/13/2006. Authors Lin and Ruan are with MOE Key Laboratory of Food Science, Nanchang Univ., Nanchang, Jiangxi 330047, China. Authors Lin, Ruan, Chen, Chung, and Ye are with Dept. of Bioproducts and Biosystems Engineering and Dept. of Food Science and Nutrition, Univ. of Minnesota, 1390 Eckles Ave., St. Paul, MN 55108, U.S.A. Authors Yang and Doona are with US Army Natick Soldier

molecules in the glassy solid state. They believe that the water in the glassy state of the starch is capable of influencing reactions at both ambient and freezing temperatures and that the glassy state of the solid material is inappropriate for predicting the molecular dynamics of water and its influence on food stability. On the other hand, Bell and others (2002), noticing the high mobility of water below the T_g , were unable to establish a clear relationship between water mobility determined by O^{17} NMR and chemical reactions and concluded that the effect of water on food chemical stability in solids is multidimensional, being dependent on the type of reaction and the physical characteristics of the system.

Water is not only the most effective plasticizer of food polymers but also an excellent solvent required for many reactions to take place in food polymers. Some researchers pointed out that the T_g theory considers mobility on a structural and macromolecular level, and, therefore, it is a parameter descriptive of the physical state of macromolecules, which differs from the molecular mobility of smaller molecules such as water (Vittadini and Chinachoti 2003). Others proposed that water activity is a solvent property, while glass transition is a property related to the structure of foods (Rahman 2005). Both properties are needed for understanding food–water relationships at different conditions (Chirife and Buera 1994). Using both the water activity and glass transition concepts in assessing process ability, deterioration, food stability, and shelf-life predictions was recommended (Roos 1995a, 1995b; Schmidt 2004).

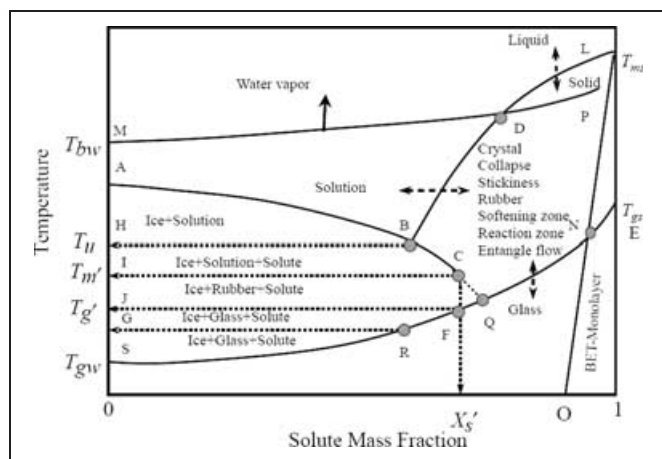


Figure 1—State diagram showing different regions and state of foods (T_{bw} , boiling point; T_u , eutectic point; T_{m0} , end point of freezing; T_{g0} , glass transition at end point of freezing; T_{gw} , glass transition of water; T_{ms} , melting point of dry solids; T_{gs} , glass transition of dry solids (Rahman and others 2003)

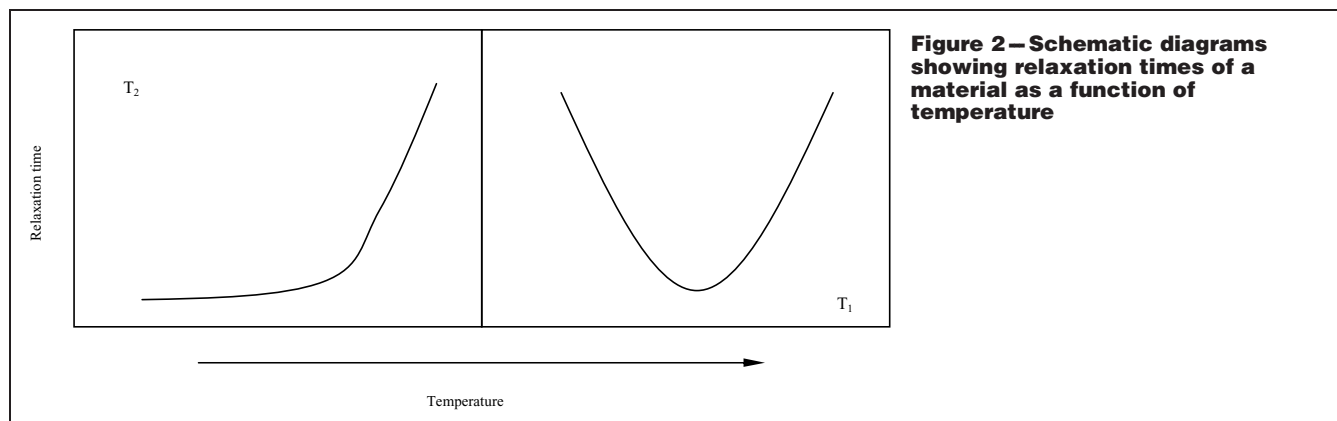


Figure 2—Schematic diagrams showing relaxation times of a material as a function of temperature

The NMR State Diagram Concept

This article demonstrates a new concept, called the NMR (nuclear magnetic resonance) state diagram, which is based on the temperature dependence of proton relaxation and physicochemical properties. An NMR state diagram is a curve of NMR relaxation time, be it spin–spin relaxation time (T_2) or spin–lattice relaxation time (T_1), versus temperature. Usually, relaxation times of liquids increase linearly with temperature. However, at very low temperatures or with solid materials, relaxation times behave drastically different. For solids, with rising temperature, T_2 changes little at low temperatures and increases rapidly above certain temperatures, characterized by a mirrored-L shape, while T_1 decreases rapidly to a certain point and rises again rapidly, characterized by a minimum (Figure 2).

Theoretical Considerations

Let us consider a high molecular weight polymer with side chain segments. When heated, some segments within the long chain of the polymer molecule are mobilized before the whole molecule starts moving. Further heating causes the entire molecule to move and become liquid. Two types of motions can be identified during the gradual heating, that is, segmental motion and molecular motion. At a certain low temperature, both motions are hindered severely or frozen; at higher temperatures, both motions may be activated. These 2 situations correspond to the solid state and liquid state, respectively. When the polymer is placed at a temperature where only the segmental motion is activated while the molecular motion is frozen, the state is called the rubbery state, and such state transition takes place at the glass–rubber transition temperature T_g . On further heating, the polymer in the rubbery state becomes a highly viscous liquid and starts flowing. The polymer moves into the viscofluid state, and such transition takes place at the flow temperature T_f . Figure 3 illustrates the relationship between motions and state transitions described earlier.

How can we relate these motions to the NMR relaxation properties? How would the detected motions behave when small molecules such as water, sugars, and so on are present? We know that NMR measures the proton relaxation characteristics, which can be related to the mobility of the proton-containing molecules. During an NMR measurement, in the time following the resonant absorption induced by a radio frequency (RF) pulse, the magnetic moments or spins of certain nuclei return to their equilibrium states or population distribution by losing energy in the form of an RF wave via various radiationless transition processes known as “relaxation processes.” The RF wave signal is characterized by the Larmor frequency of the nucleus, and can be received and recorded by the NMR instrument (an RF receiving antenna). There are 2 kinds of relaxation

processes: spin–lattice (or longitudinal) relaxation and spin–spin (or transverse) relaxation. The time constants describing these exponential relaxation processes are known as relaxation times. The spin–lattice relaxation time is designated by T_1 and the spin–spin relaxation time is designated by T_2 . Relaxation time is a function of the spin species and the chemical and physical environments surrounding the spins. Therefore, analysis of T_1 and T_2 of a sample will allow the study of the chemical and physical properties of the sample. A long T_1 or T_2 indicates a slow relaxation and a short T_1 or T_2 value indicates a rapid relaxation.

The dynamic motion of spins can be characterized by a correlation time τ_c , which is, roughly speaking, the minimum time required for the nuclear magnetic moment to rotate 1 radian ($\frac{1}{2}\pi$ of a complete circle). In general, τ_c for nonviscous liquid is very short. With water, for instance, τ_c is about 10^{-12} s. On the other hand, τ_c for solids is very long, about 10^{-5} s. Within limits, the slower the motion, the longer the τ_c , and the faster a perturbed spin system will relax. Thus, the relationship between the motional characteristics and NMR relaxation can be established through the relationship between τ_c and relaxation time, as described in Eq. 1 and 2 (Farrar 1989):

$$\frac{1}{T_1} = K \left[\frac{\tau_c}{1 + (\omega_0 \tau_c)^2} + \frac{4\tau_c}{1 + (2\omega_0 \tau_c)^2} \right] \quad (1)$$

$$\frac{1}{T_2} = \frac{K}{2} \left[3\tau_c + \frac{5\tau_c}{1 + (\omega_0 \tau_c)^2} + \frac{2\tau_c}{1 + (2\omega_0 \tau_c)^2} \right] \quad (2)$$

where $K = \frac{3\mu^2}{160\pi^2} \frac{\hbar^2 \gamma^4}{r^6}$ is a constant that includes a number of nuclear parameters and constants, and ω_0 is the resonance frequency. Figure 4 is a plot of τ_c versus relaxation time constants T_1 and T_2 . The curves are similar to those in Figure 1 (Ruan and Chen 1998). This is because, within limits, τ_c is related to temperature. Their relationship can be described by Eq. 3:

$$\tau_c = \tau_{c0} e^{E_{act}/kT} \quad (3)$$

where E_{act} is the activation energy for rotational motion, k the Boltzmann constant, T the absolute temperature, and τ_{c0} is a constant.

Fundamentally, T_1 , T_2 , and Eq. 1 and 2 describe the rotational motions of nuclei. It is understood that translational motion occurs in liquid and gas phases of water and is limited in low-moisture foods but virtually ceases to exist in solid phase of water (Schmidt 2004). It is suggested that rotation of a probe molecule (e.g., water) in a viscous liquid should be coupled to the structural relaxation of the surroundings, which is largely determined by the translational diffusion properties and the structure of the neighboring molecules (Bagchi 2001). The fact that the product of correlation time and

translational diffusion coefficient is a constant indicates that rotational and translational motions are closely related (Bagchi 2001; Netz and others 2002). Netz and others (2002) suggest that translational and rotational motions are controlled by a common mechanism. Therefore, T_1 and T_2 are conveniently coupled to molecular mobility; however, the relationship between relaxation times and molecular mobility depends on the nucleus being probed and surrounding systems (Belton and others 1995; Schmidt 2004). Such a relationship could be very complicated in complex food systems, and therefore additional relaxation mechanisms such as chemical exchange, diffusion exchange, cross-relaxation, and paramagnetic relaxation may also contribute to the relationship (Schmidt 2004).

Figure 5 shows a plot of $\ln(T_2)$ versus reciprocal temperature ($1/T$) for a pure biodegradable polymer PLA (polylactic acid). The relaxation data obtained using a 90° RF pulse were fitted well into a single exponential equation at temperatures below 75°C and a bi-exponential equation at temperatures above 75°C . The plot shows

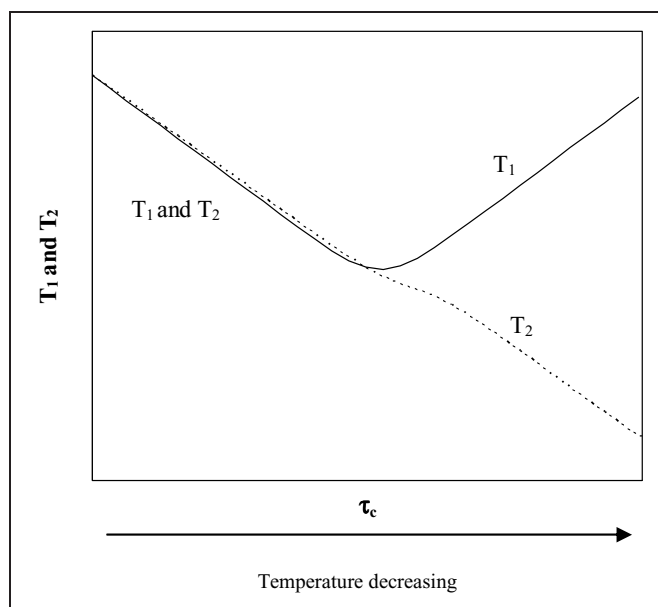


Figure 4 – A generalized schematic diagram showing the relationships between relaxation time constants and correlation time

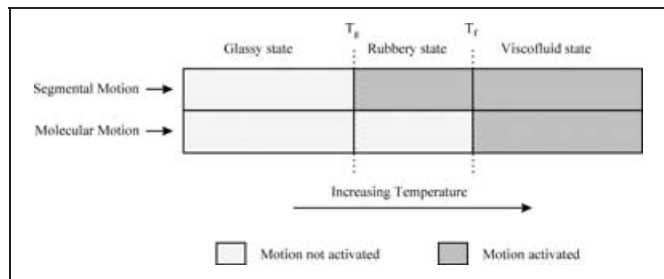


Figure 3 – A schematic presentation of the relationship between states and motional characteristics of a polymer. T_g , glass transition temperature; T_f , flow temperature

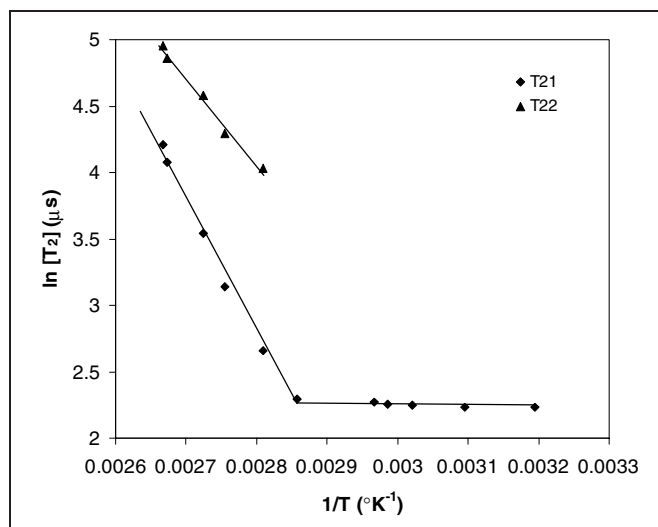


Figure 5 – Relationship between spin–spin relaxation time (T_2) and temperature in PLA

a clear transition with the transition temperature ($\sim 75^\circ\text{C}$) being very close to its glass transition temperature (70°C) measured with DSC. At temperature below 75°C , T_{21} is independent of temperature. Above 75°C , T_{21} begins to increase rapidly with increasing temperature. Our observation is in agreement with that observed in amylopectin by Kalichevsky and others (1992), who attributed the increase in relaxation time to the onset or increase in frequency of the motion of groups containing hydrogen. Figure 6 shows the similar type of plot for maltodextrins at different moisture or solid fraction levels (Ruan and others 1999). Yoshioka and coworkers (Yoshioka and others 1997, 1999; Yoshioka and Aso 2004) reported similar plots obtained for freeze-dried γ -globulin formulations. In their studies, the transition temperatures on the temperature- T_2 curves were defined as critical mobility temperature (T_{mc}), which were generally lower than T_g measured by DSC, indicating that T_{mc} represents the temperature at which the molecular mobility begins to increase in a temperature range lower than the T_g determined by DSC. They concluded that T_{mc} determined by NMR is more sensitive to protein stability than T_g determined by DSC.

Figure 6 shows several noteworthy features. First, the transition temperature decreased as moisture content increased, which is a characteristic of glass transition temperature. Second, the T_2 level increased with increasing moisture content, regardless of whether the material is below or above the state transition temperature, suggesting that there are motions even below the transition temperature. Third, the slopes of the two linear phases of each curve tend to increase slightly with increasing moisture content. These three features, namely the transition temperature, the T_2 level, and the slopes, may provide additional information on the state of a polymeric system, which, in principle, should help understand the physical, structural, chemical, and biological changes associated with state transition and presence of water or other plasticizers.

Experimental Evidence

Although the data presented earlier illustrated some interesting features of the NMR state diagram, which appears to be related to the physiochemical states of food polymers, direct evi-

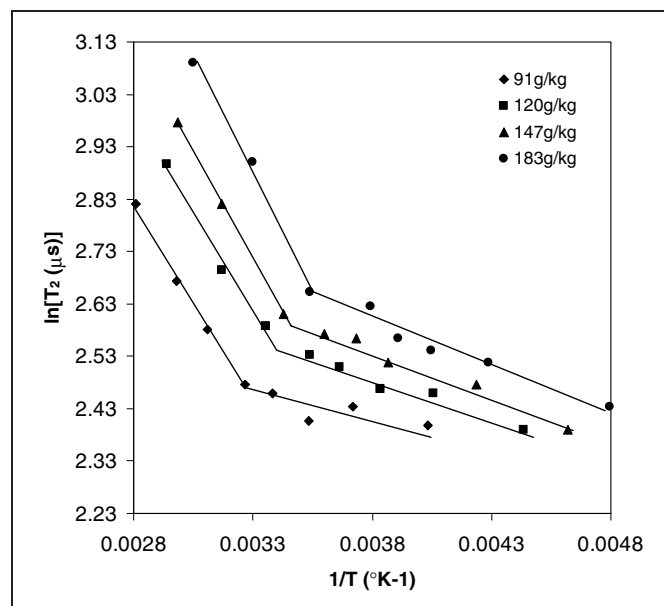


Figure 6 – Relationship between spin-spin relaxation time (T_2) and temperature (T) in maltodextrins (DE15). The legend indicates the grams of water in the 1 kg maltodextrins.

dence to show the correlations between these features and physical changes and chemical and biological reactions in food systems is essential to the verification and improvement of the concept. The data presented below demonstrate how the NMR state diagram concept could be applied to situations where changes in food quality properties were due to physiochemical changes, while more data on chemical and biological activities are being sought.

Caking of dry powders

Glass transition is believed to influence caking of dry powders (Noel and others 1990; Roos and Karel 1991; Wallack and King 1998). Particles of powders may stick together if sufficient liquid is available to plasticize the surface of the particles so that “bridges” can be formed between them (Peleg 1993; Aguilera and others 1995). The rate of caking is believed to be mainly governed by Peleg (1993), Aguilera and others (1995):

$$\Delta T = T - T_g \quad (4)$$

where T is the storage temperature, and ΔT is the difference between the storage temperature and the glass transition temperature. Eq. 4 indicates that the product will have different length of shelf-life if stored at different temperatures, depending on how far the storage temperatures are from the T_g . However, our study shows dry powders may cake when stored below state transition temperature and may not cake when stored above state transition temperature within the timeframe of the experiments (Chung and others 2000). It is known that caking is time-dependent (Aguilera and others 1993). If there is mobility in the system stored either below or above the state transition temperature, physiochemical changes could take place to an extent sufficient to cause caking if given sufficient time.

In a study (Chung and others 2000) of caking of dry powdered ingredients (Figure 7) during storage, we acquired the T_2 values of these ingredients during temperature scans between -20°C and 120°C and obtained the temperature- T_2 curves as shown in Figure 7. We found that the shapes of temperature- T_2 curves fell into 4 patterns, as illustrated in Figure 8. A dotted line is drawn to divide each curve into 2 portions as shown in Figure 8. The portion on the left side of the dotted line corresponds to before-transition changes in T_2 , and the portion on the right side of the dotted line corresponds to posttransition changes in T_2 as a function of temperature. The slope for the before-transition phase is denoted as k_{BT} and the slope for the posttransition phase as k_{PT} . Table 1 shows whether the curve has a transition temperature and whether k_{BT} and k_{PT} are approximately equal to or greater than zero. A nonzero k_{BT} or k_{PT} indicates that the molecular or segmental movements in the samples increased as the temperature was increased. We would like to emphasize that a greater than zero k_{BT} suggests that there is mobility even below the state transition temperature, and this mobility could be high enough for physical, chemical, and biological changes to take place even at the glassy state.

During the temperature scans, 2 types of changes in relation to caking of the samples were observed: Type I: slow and gradual agglomeration and water vaporization, and Type II: abrupt caking. We found that a transition on the temperature- T_2 curve (Patterns A and B) coincides with the occurrence of Type II change, and a greater-than-zero k_{BT} (Patterns A and C) coincides with the occurrence of Type I change. No Type I or Type II changes occurred to the samples with a straight line parallel to the x-axis (Pattern D).

To establish the relationship between caking and the parameters obtained from the curves, we observed and measured the caking characteristics of all the samples during 60 d of storage at 37°C and 55°C (Table 2). Most of samples in Group A caked even when stored

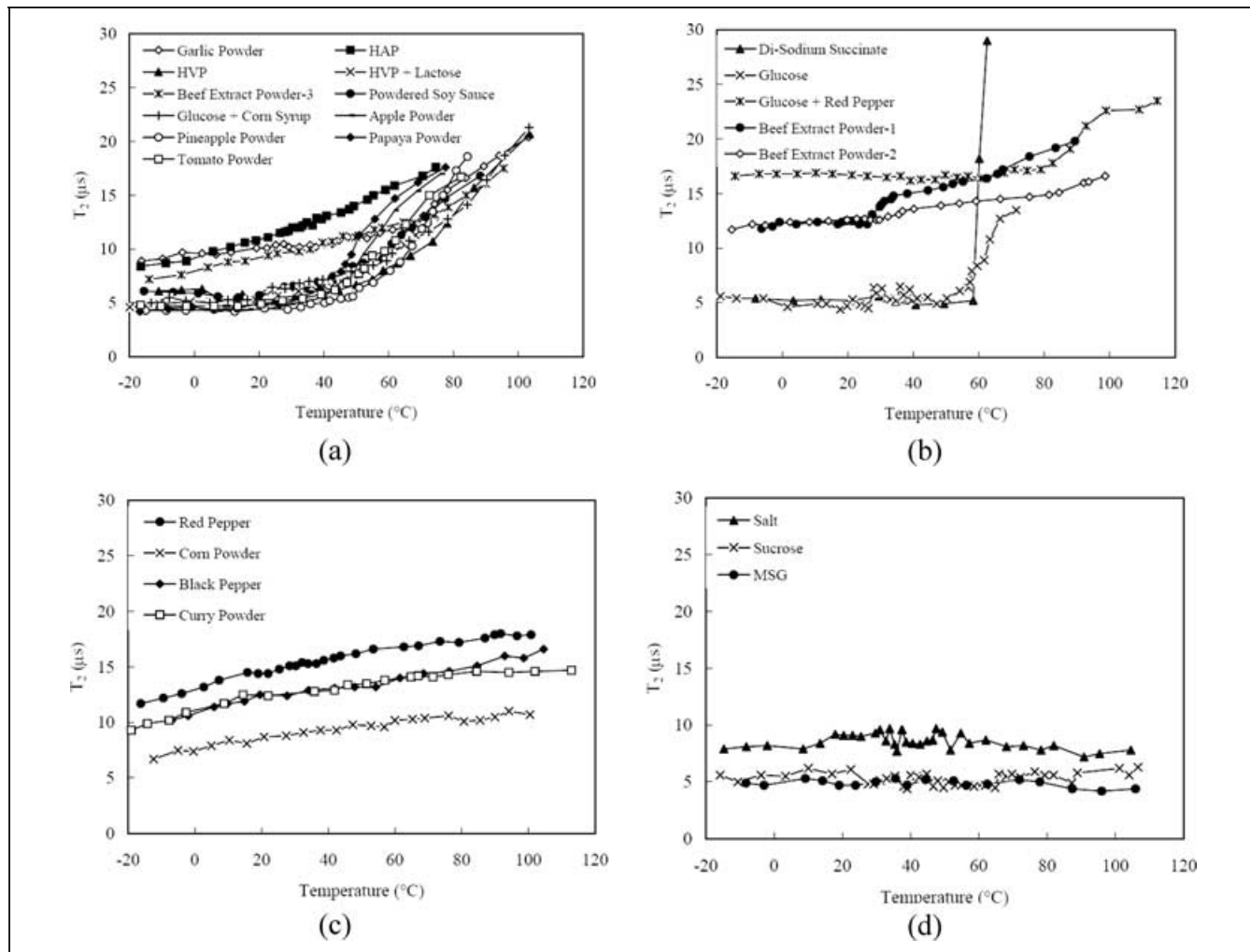


Figure 7 – T_2 (spin-spin relaxation time constant) changes as a function of temperature for powdered ingredients (Chung and others 2000)

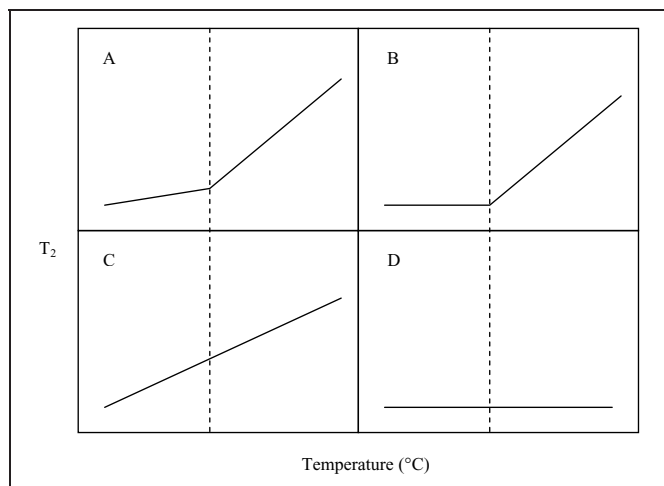


Figure 8 – Schematic demonstration of four different temperature- T_2 curve patterns for the dry soup powders

below their transition temperatures. All those samples that did not cake within the storage timeframe were characterized with zero or very low slopes or without a transition temperature. These results indicate that a nonzero k_{BT} , a relatively high k_{PT} , and the presence of a transition temperature were all necessary for caking to take

Table 1 – Significant features of temperature- T_2 curves for dry soup mixes (Chung and others 2000)

Pattern	T_{Tran}	k_{BT}	k_{PT}
A	Yes	> 0	> 0
B	Yes	≈ 0	> 0
C	No	> 0	> 0
D	No	≈ 0	≈ 0

See text for explanation.

place within the storage timeframe, while whether the samples were stored below or above the transition temperature is less critical. A multiple regression model (Eq. 2) based on the NMR state diagram parameters was able to fit into the data very well (Chung and others 2000).

$$DUC = \text{constant} + a \cdot T_{Tran} + b \cdot k_{BT} + c \cdot k_{PT} + bc \times k_{BT} \cdot k_{PT} \quad (5)$$

where DUC is days until caking; a , b , and c are main effects of $\Delta T = T - T_{Tran}$, k_{BT} and k_{PT} , respectively; and bc is an interaction effect of k_{BT} and k_{PT} .

Equation 5 also suggests the feasibility of using this concept to predict caking resistance and formulate soup powders with desirable caking resistance. Chung and others (2003) were able to demonstrate that the state diagram curve pattern of a mixture of two

Table 2—Parameters for each powder estimated by NMR experiments and results of storage tests

Classification	Powder	T_{Trans} (°C)	k_{BT} ($\mu\text{s}/^\circ\text{C}$) ^a	k_{PT} ($\mu\text{s}/^\circ\text{C}$) ^b	Days until Caking	
					37 °C	55 °C
A	Garlic powder	60	0.03	0.16	—	—
	HAP	32	0.08	0.13	—	—
	HVP	61	0.05	0.39	—	0.5
	HVP + lactose	45	0.03	0.20	24	0.3
	Beef extract powder-3	69	0.06	0.18	—	2
	Powdered soy sauce	59	0.09	0.29	—	1.3
	Glucose + corn syrup	63	0.07	0.33	20	0.5
	Apple powder	42	0.11	0.35	14	0.1
	Pineapple powder	50	0.08	0.45	2	0.02
	Papaya powder	45	0.15	0.35	19	0.2
	Tomato powder	50	0.14	0.29	25	0.6
B	Disodium succinate	58	0.00	5.00	—	—
	Glucose	58	0.00	0.55	—	—
	Glucose + red pepper	68	0.00	0.16	—	—
	Beef extract powder-1	27	0.00	0.12	—	—
	Beef extract powder-2	31	0.00	0.06	—	—
C	Red pepper	N.T.	0.05	0.05	—	—
	Corn powder	N.T.	0.03	0.03	—	—
	Black pepper	N.T.	0.05	0.05	—	—
	Curry powder	N.T.	0.04	0.04	—	—
D	Salt	N.T.	0.00	0.00	—	—
	Sucrose	N.T.	0.00	0.00	—	—
	Mono-sodium glutamate	N.T.	0.00	0.00	—	—

N.T. – no transition.

or more powder ingredients was governed and could be predicted by the curve patterns of the individual powders. Figure 9 shows the curve patterns of 6 mixtures of 2 powders having different curve patterns as a function of the mixing ratio. Powder disodium succinate (DSS) exhibits a Pattern B curve, while hydrolyzed animal protein (HAP) shows a Pattern A curve. When they were mixed at different ratios, the mixtures show a series of Pattern A curves with different T_{Trans} , k_{BT} , and k_{PT} (Figure 10). Keeping in mind that Pattern A powders are more susceptible to caking than Pattern B powders (Chung and others 2000), we expect that an increase in DSS in the mixture should enhance the caking resistance of the mixture. As Figure 9 shows, we observed that the transition temperature shifted to the right as DSS was increased. The quantitative analysis shows that the transition temperature increased linearly with increasing DSS (Figure 10a), k_{BT} decreased rapidly with increasing DSS in the low DDS range, and k_{PT} increased rapidly with increasing DSS in the high DSS range (Figure 10b). By varying the amount of ingredients having different susceptibilities to caking, it is possible to formulate products with a designed shelf-life, which was supported by the results from Chung and others (2001). Increasing the proportions of caking-resistant ingredients in soup recipes lowered the caking tendency without using an anticaking agent, which has tremendous commercial value.

Firming of model high-protein bars

Figure 11 shows the change in hardness of 2 model high-protein bar samples containing primarily proteins, some carbohydrates, and other minor ingredients (Table 3). The 2 samples differed mainly in protein composition; that is, Sample A contained 27.6% P0320 and 6.9% P0313, while Sample B contained only P0313 (34.4%). Sample B was harder and firmed more rapidly than Sample A. The changes in a_w and moisture as a function of storage time are shown in Table 4. Sample A had slightly lower moisture content and a_w than Sample B. Both a_w and moisture content changed very little and fluctuated during the storage. The changes in hardness were found to correlate poorly with changes in moisture content and water activity during the storage. This seems to suggest that firming of the bars was not due to moisture loss, and water activity was not sen-

sitive enough to reflect the changes in the physiochemical states of the samples. Our NMR study showed that the protons in Sample B (hard) were generally less mobile than those in Sample A (soft). The mobility of both samples decreased with increasing storage time, which was coincident with the texture-firming phenomenon. Figure 12 shows that Sample B had a higher T_{Trans} , k_{BT} , and k_{PT} than Sample A, which may contribute to the faster firming of Sample B.

We took a similar approach to that used in the caking study described earlier to screen the NMR state diagrams of 10 proteins, 4 sugar alcohols, 7 protein-sugar alcohol mixtures, and 1 model high protein bar. The results, shown in Figure 13 to 18, indicate that the curve shapes for the individual protein samples can be classified into 3 of the 4 types described earlier in this article:

Type I (Figure 13, Pattern A): a gradual initial increase followed by a more rapid increase after a transition point, Proteins 4, 5, 6, and 7.

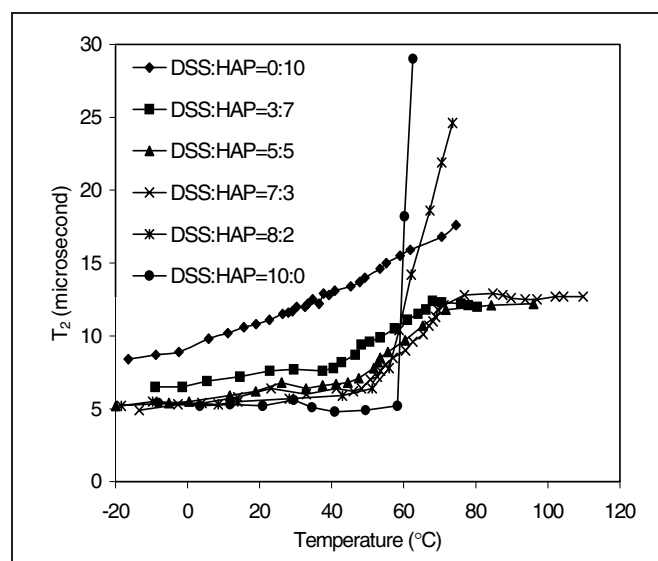
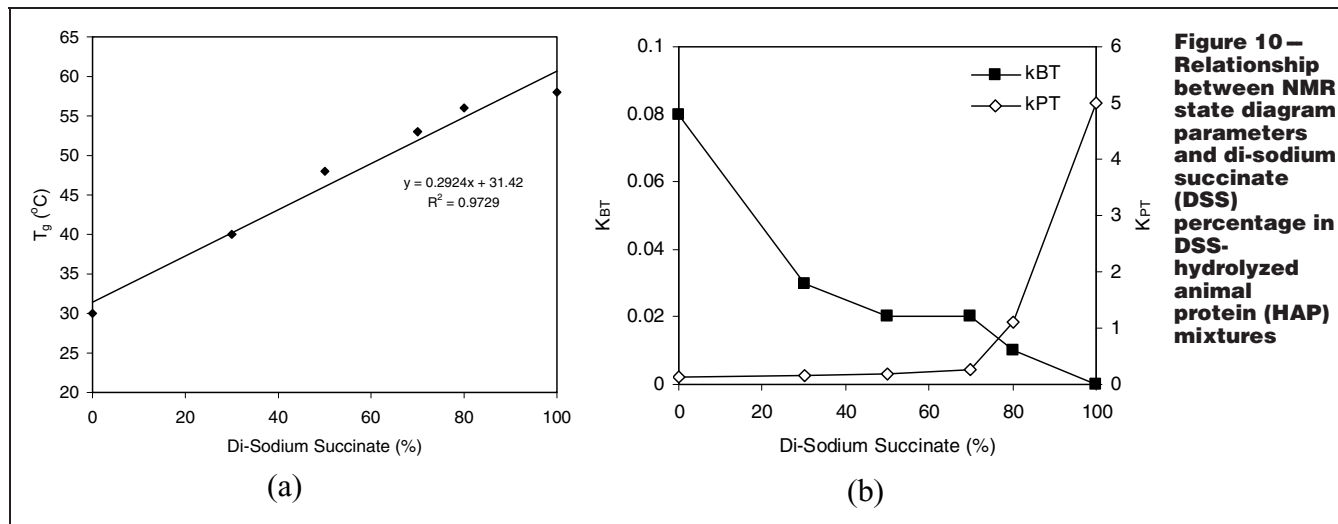


Figure 9— T_2 changes as a function of temperature for di-sodium succinate (DSS) and hydrolyzed animal protein (HAP) mixtures



Type II (Figure 14, Pattern B): a steady initial stage followed by a rapid increase after a transition point, Proteins 2, 3, and 9.

Type IV (Figure 15, Pattern D): no apparent change in trend within the tested temperature range, Proteins 1, 8, and 10.

According to our findings from the caking study, Type I samples are less stable than Type II and Type IV samples; Protein 5 would be expected to be the least stable, and Protein 1 would be expected to be the most stable.

For the sugar alcohols (Figure 16), the curve shapes are different from those of proteins. Since there is no prior experience or reports on the state diagrams of liquid samples, it was expected that sorbitol would be the most mobile, while glycerin would be the least mobile among the liquid sugar alcohols.

To investigate how the curve patterns of individual proteins and sugar alcohols predict the curve patterns of mixtures, we mixed Protein 1 with different sugar alcohols. Figure 17 shows the temperature- T_2 curves of these mixtures. The general trend tends to agree with the mobility of individual sugar alcohols shown in Figure 16, with Protein 1/sorbitol being predicted to be less stable than Protein 1-polydextose mixture and Protein 1-maltitol mixture. The model bar would be expected to be the most unstable.

We further evaluated the effect of water activity on the curve pattern of protein-sugar alcohol mixtures. Figure 18 shows that the temperature- T_2 curves for Protein 1-glycerin mixtures shifted upwards as the water activity increased, especially when a_w was above 0.4. The upward shift is expected to be associated with decreased stability.

Studies of the main and interaction effects of proteins on textural changes and the relationships between these effects and NMR relaxation properties using binary, ternary, and quaternary model systems are under way. The objective is to use NMR relaxometry and the state diagram concept as a tool to screen proteins and develop models for predicting shelf-life stability of high-protein bars. The outcome of the studies would greatly enhance our ingredient screening and development capability.

Chemical reactions and microbial stability

Our previous experiments provide good validation support to the NMR state diagram concept when applied to physical changes. Data on the relationship between the NMR state diagram and the chemical reactions and microbial stability in food products are highly desirable if we want to extend the concept to chemical and biological changes in foods. Experiments employing amorphous glassy models to study the effect of glass transition and NMR relaxation properties

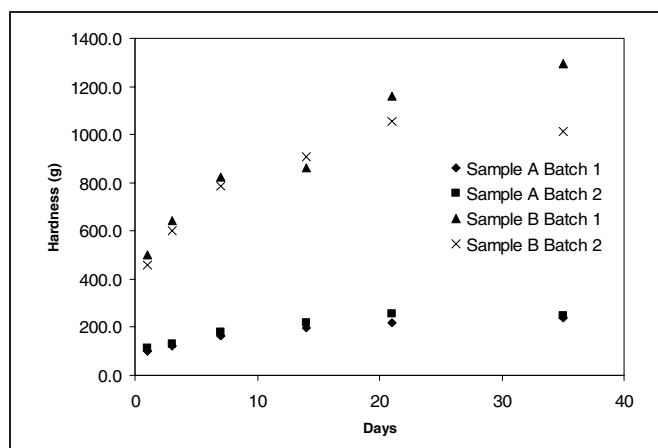


Figure 11 – Firming of 2 high-protein bar samples during storage

Table 3 – Composition of 2 model protein bars

Ingredient	Sample A (%)	Sample B (%)
Isolated soy protein, FXP H0320	27.6	
Isolated soy protein, FXP H0313	6.9	34.4
Rice syrup solids, 26 DE	7.7	7.8
Cocoa powder	5.1	5.1
Vitamin and mineral premix	0.7	0.7
Salt	0.1	0.1
Corn syrup, 63 DE	26.1	26.1
High fructose corn syrup, 55% fructose	21.3	21.3
Glycerin (99.7%)	3.9	3.9
Chocolate flavor A	0.3	0.3
Chocolate flavor B	0.3	0.3
Vanilla flavor	0.1	0.1
Total	100.0	100.0

on Maillard reactions are under way. This study may shed some light on the separate roles of water mobility and structural mobility in the stability of food products.

NMR Methodology

The methods for most of experiments described in this article can be found in the references cited. The methodology described here was used for experiments involving PLA and protein bars. The NMR experiments were performed on a MARAN DRX bench top imager with a high quality permanent magnet of 21.4 MHz

Table 4 – Changes in a_w and moisture content of two model protein bars during storage.

Days	a_w				Moisture Content			
	Sample A		Sample B		Sample A		Sample B	
	Batch 1	Batch 2	Batch 1	Batch 2	Batch 1	Batch 2	Batch 1	Batch 2
1	0.471	0.480	0.483	0.504	11.20	11.50	11.50	11.70
3	0.473	0.461	0.478	0.478	10.60	10.50	10.60	10.80
7	0.468	0.458	0.483	0.494	11.10	11.10	11.80	11.70
14	0.464	0.443	0.479	0.469	10.90	11.00	11.40	11.40
21	0.478	0.477	0.488	0.484	11.50	11.50	11.70	12.00
35	0.412	0.418	0.467	0.443	11.40	11.40	12.30	11.30
Mean	0.461	0.456	0.480	0.479	11.13	11.17	11.55	11.48

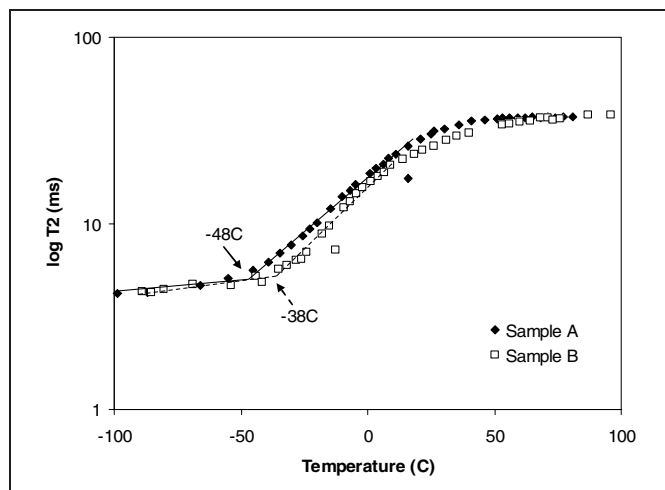


Figure 12 – NMR state diagram of two high-protein bar samples

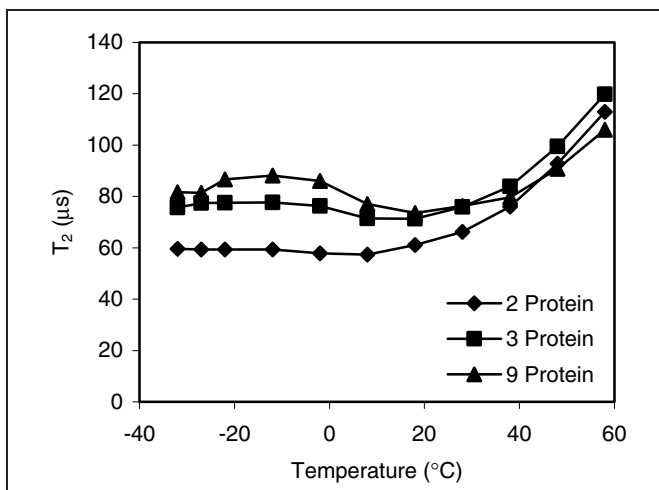


Figure 14 – T_2 as a function of temperature (individual proteins – Type B)

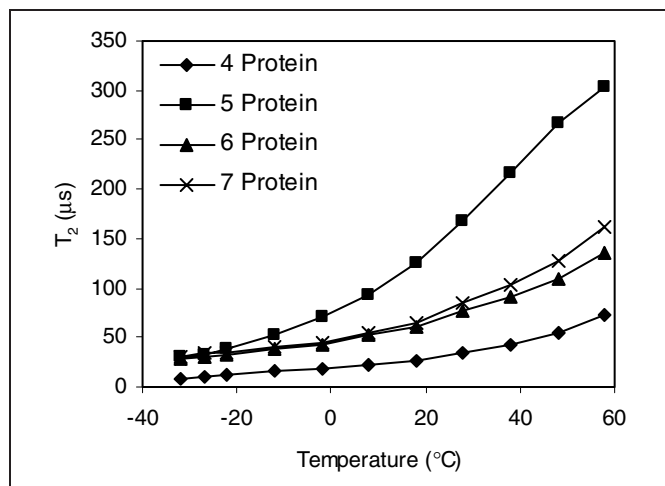


Figure 13 – T_2 as a function of temperature (individual proteins – Type A)

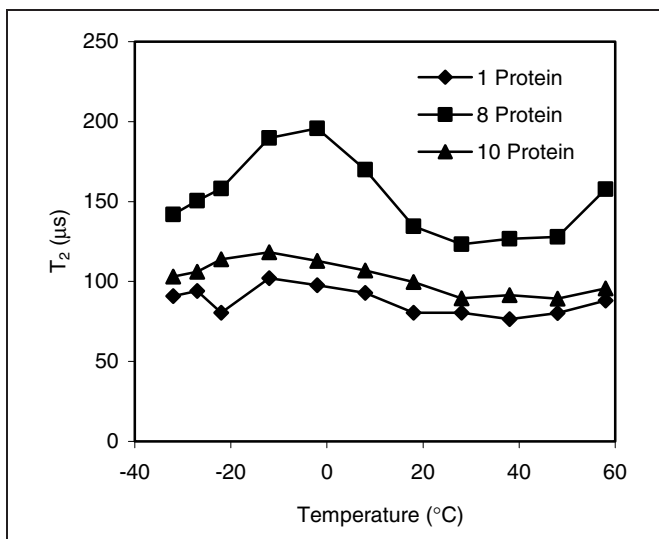


Figure 15 – T_2 as a function of temperature (individual proteins – Type D)

proton resonance frequency (Resonance Instruments Ltd., Witney, Oxon, U.K.). Spin-spin relaxation time (T_2) measurements were performed with the a 90° RF pulse. For all NMR experiments, a sample relaxation delay of 5 s ($\geq 5 T_1$), a 90° pulse of $9 \mu s$, and 2 consecutive scans were used. The NMR relaxation data were fitted to a single exponential decay and a 2-exponential function using the RI WinFit software provided by the vendor.

Implications

The NMR state diagram concept may help understand the effect of mobility of macrostructure, small solutes, and water on

physical, chemical, and biological changes in food products. The potential applications of the concept may include (1) ingredients screening, useful for product formula development; (2) prediction of physiochemical changes (texture, viscosity, caking, water and fat migration, and so on), chemical degradation of nutrients, and microbiological activity, which are associated with mobility of water and polymers; and (3) combined with magnetic resonance imaging (MRI) techniques, the concept would greatly improve our understanding of quality and safety of food products, especially intermediate moist foods (IMF).

Further research is needed to develop methodology to determine the mobility of individual components and its relation to shelf stability. Some researchers suggest that it is necessary to determine the mobility of reactants in addition to the mobility of physical structure

and water in order to directly quantify the relationship between reactions and molecular mobility (Sherwin and others 2002). Others (Tolstoguzov 2000) suggest that there are nonwater plasticizers in food polymers whose effects on molecular mobility must be considered as an important factor in food stability.

More in-depth studies to analyze the relationships among NMR relaxation, molecular mobility, and stability of foods are necessary. Combination of the NMR state diagram concept, the a_w concept, and the glass transition concept is a preferred approach to the study of relationships between mobility and shelf stability of food products (Ross 1995a, 1995b; Schmidt 2004).

Acknowledgment

This work was supported by China Ministry of Education PCSIRT Program (IRT0540), Minnesota Agricultural Experiment Station, and private donations.

References

Aguilera JM, Levi G, Karel M. 1993. Effect of water content on the glass transition and caking of fish protein hydrolyzates. *Biotechnol Prog* 9(6):651-4.

Aguilera JM, del Valle JM, Karel M. 1995. Caking phenomena in amorphous food powders. *Trends Food Sci Technol* 6:149-55.

Bagchi B. 2001. Relation between orientational correlation time and the self-diffusion coefficient of tagged probes in viscous liquids: a density functional theory analysis. *J Chem Phys* 115(5):2207-11.

Bell LN, Hageman MJ. 1994. Differentiating between the effects of water activity and glass transition dependent mobility on a solid state chemical reaction: aspartame degradation. *J Agric Food Chem* 42(11):2398-401.

Bell LN, Bell HM, Glass TE. 2002. Water mobility in glassy and rubbery solids as determined by oxygen-17 nuclear magnetic resonance: impact on chemical stability. *Lebens Wissens Technol* 35(2):108-13.

Belton PS, Delgado I, Gil AM, Webb GA. 1995. *Magnetic resonance in food science*. Cambridge, U.K.: Royal Society of Chemistry.

Buera MP, Karel M. 1995. Effect of physical changes on the rates of nonenzymic browning and related reactions. *Food Chem* 52(2):167-73.

Buera MP, Jouppila K, Roos YH, Chirife J. 1998. Differential scanning calorimetry glass transition temperatures of white bread and mold growth in the putative case. *Cereal Chem* 75:64-9.

Chirife J, Buera MP. 1994. Water activity, glass transition and microbial stability in commercial/semimoist food systems. *J Food Sci* 59:921-7.

Chirife J, Buera MP. 1995. A critical review of some non-equilibrium situations and glass transition on water activity of foods in the microbiological growth range. *J Food Eng* 25:531-52.

Chirife J, Buera MP. 1996. Water activity, water glass dynamics, and the control of microbiological growth in foods. *Crit Rev Food Sci Nutr* 36:465-513.

Chung MS, Ruan R, Chen P, Lee YG, Ahn TH, Baik CK. 2001. Formulation of caking-resistant powdered soups based on NMR analysis. *J Food Sci* 66(8):1147-51.

Chung MS, Ruan RR, Chen P, Chung SH, Ahn TH, Lee KH. 2000. Study of caking in powdered foods using nuclear magnetic resonance spectroscopy. *J Food Sci* 65(1):134-8.

Chung MS, Ruan R, Chen P, Jin-Ho K, Tae-Hoi A, Chang-Kyu B. 2003. Predicting caking behaviors in powdered foods using a low-field nuclear magnetic resonance (NMR) technique. *Lebens Wissens Technol* 36(8):751-61.

Farrar TC. 1989. *Pulsed NMR spectroscopy*. Madison: The Farragut Press. p 211.

Kalichevsky MT, Jaroszkiewicz EM, Ablett S, Blanshard JMV, Lillford PJ. 1992. The glass transition of amylopectin measured by DSC, DMTA and NMR. *Carbohydrate Polymers* 18(2):77-88.

Kilcast D, Subramaniam P. 2000. *The stability and shelf-life of food*. Cambridge, U.K.: Woodhead Publishing.

Li S, Dickinson LC, Chinachoti P. 1998. Mobility of unfreezable and freezable water in waxy corn starch by 2H and 1H NMR. *J Agric Food Chem* 46(1):62-71.

Nelson KA. 1994. Reaction kinetics of food stability: comparison of glass transition and classical models for temperature and moisture dependence [PhD diss]. Dept. of Food Science and Nutrition, Univ. of Minnesota, St. Paul.

Netz PA, Starr F, Barbosa MC, Stanley HE. 2002. Translational and rotational diffusion in stretched water. *J Mol Liquids* 101:159-68.

Noel TR, Ring SG, Whittam MA. 1990. Glass transitions in low-moisture foods. *Trends Food Sci Technol* 1:62-7.

Peleg M. 1993. Glass transitions and the physical stability of food powders. In: Blanshard JMV, Lillford PJ, editors. *The glassy state in foods*. Nottingham, U.K.: Nottingham Univ. Press. p 435-51.

Rahman MS. 2006. State diagram of foods: its potential use in food processing and product stability. *Trends Food Sci Technol* 17(3):129-41.

Rahman MS, Kasapis S, Guizani N, Al-Amri OS. 2003. State diagram of tuna meat: freezing curve and glass transition. *J Food Eng* 57(4):321-6.

Roos Y. 1995a. Characterization of food polymers using state diagrams. *J Food Eng* 24:339-60.

Roos Y. 1995b. Water activity and glass transition temperature: How do they complement and how do they differ? In: Barbosa-Canovas GV, Welti-Chanes J, editors. *Food preservation by moisture control: fundamentals and applications*. Pa.: Technomic. p 133-54.

Roos Y, Karel M. 1991. Applying state diagrams to food processing and development. *Food Technol* 45(12):66, 68-71, 107.

Roos YH, Karel M, Kokini JL. 1996. Glass transitions in low moisture and frozen foods: effects on shelf life and quality. *Food Technol* 50(11):95-108.

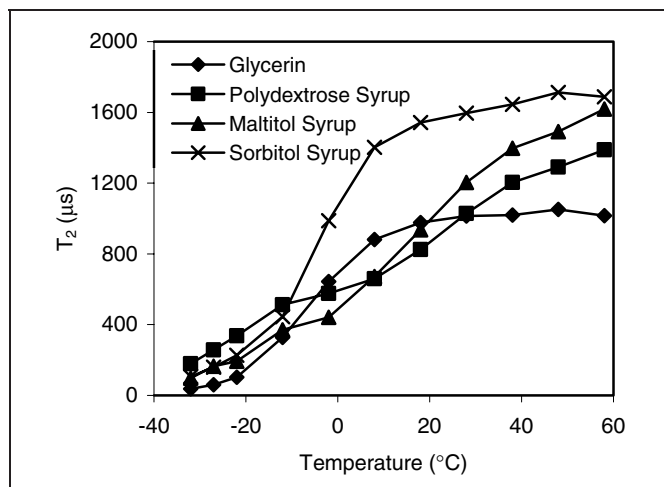


Figure 16— T_2 as a function of temperature (individual sugar alcohols)

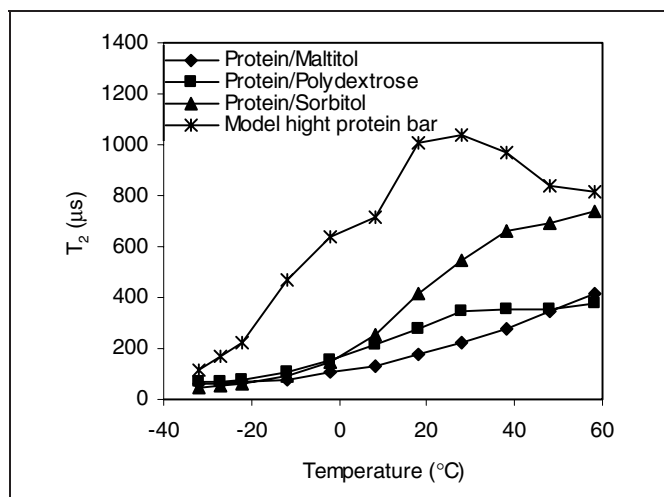


Figure 17— T_2 as a function of temperature protein-sugar alcohol mixtures and a model high-protein bar

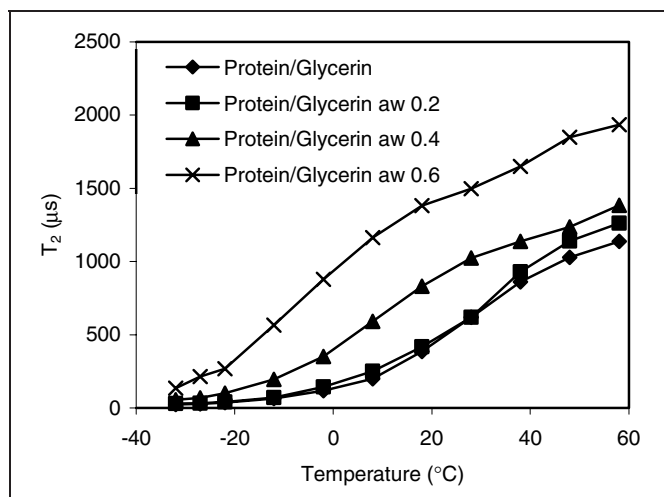


Figure 18— T_2 as a function of temperature protein-glycerin mixtures at different a_w

- Roudaut G, Maglione M, Dusschoten DV, Meste ML. 1999. Molecular mobility in glassy bread: a multispectroscopy approach. *Cereal Chem* 76(1):70–7.
- Ruan RR, Chen PL. 1998. Water in foods and biological materials: a nuclear magnetic resonance approach. Lancaster, Pa.: Technomic Publishing Co.
- Ruan R, Long Z, Chen P, Huang V, Almaer S, Taub I. 1999. Pulse NMR study of glass transition in maltodextrin. *J Food Sci* 64(1):6–9.
- Schmidt SJ. 2004. Water and solids mobility in foods. *Adv Food Nutr Res* 48:1–101.
- Sherwin CP, Labuza TP, McCormick A, Bin C. 2002. Cross-polarization/magic angle spinning NMR to study glucose mobility in a model intermediate-moisture food system. *J Agric Food Chem* 50(26):7677–83.
- Slade L, Levine H, Ievolella J, Wang M. 1993. The glassy state phenomenon in applications for the food industry: application of the food polymer science approach to structure-function relationships of sucrose in cookie and cracker systems. *J Sci Food Agric* 63(2):133–76.
- Tolstoguzov VB. 2000. The importance of glassy biopolymers components in food. *Nahrung* 44(2):76–84.
- Vittadini E, Chinachoti P. 2003. Effect of physico-chemical and molecular mobility parameters on *Staphylococcus aureus* growth. *Int J Food Sci Technol* 38:841–7.
- Yoshioka S, Aso Y. 2004. Glass transition-related changes in molecular mobility below glass transition temperature of freeze-dried formulations, as measured by dielectric spectroscopy and solid state nuclear magnetic resonance. *J Pharm Sci* 94(2):275–87.
- Yoshioka S, Aso Y, Kojima S. 1997. Dependence of the molecular mobility and protein stability of freeze-dried r-globulin formulations on the molecular weight of dextran. *Pharm Res* 14(6):736–41.
- Yoshioka S, Aso Y, Kojima S. 1999. The effect of excipients on the molecular mobility of lyophilized formulations, as measured by glass transition temperature and NMR relaxation-based critical mobility temperature. *Pharma Res* 16(1):135–40.
- Wallack DA, King CJ. 1988. Sticking and agglomeration of hygroscopic, amorphous carbohydrate and food powders. *Biotechnol Prog* 4(1):31–5.